Electron spin polarization in resonant interband tunneling devices

A. G. Petukhov,[1,2] D. O. Demchenko,[1,*] and A. N. Chantis[1,†]
[1]*Physics Department, South Dakota School of Mines and Technology, Rapid City, South Dakota 57701, USA*
[2]*Center for Computational Materials Science, Naval Research Laboratory, Washington, DC 20375, USA*
(Received 9 July 2003; published 29 September 2003)

We study spin-dependent interband resonant tunneling in double-barrier InAs/AlSb/ $Ga_xMn_{1-x}Sb$ heterostructures. We demonstrate that these structures can be used as spin filters utilizing spin-selective tunneling of electrons through the light-hole resonant channel. High densities of the spin-polarized electrons injected into bulk InAs make spin-resonant tunneling devices a viable alternative for injecting spins into a semiconductor. Another striking feature of the proposed devices is the possibility of inducing additional resonant channels corresponding to the heavy holes. This can be implemented by saturating the in-plane magnetization in the quantum well.

DOI: 10.1103/PhysRevB.68.125332 PACS number(s): 73.40.Gk, 75.50.Pp, 85.75.Mm

One of the goals and challenges of the modern spintronics is the ability to create stable sources of spin-polarized electrons that can be injected into the bulk of a semiconductor. One way of achieving this goal is to inject spins from a ferromagnetic metal into a semiconductor through a Schottky barrier.[1–3] Another alternative consists in using all-semiconductor spin filtering devices. One class of the proposed spin filters utilizes the Rashba effect in double-well resonant tunneling structures.[4] Another class of these devices uses interband (or Zener) spin-dependent tunneling in heterostructures comprising nonmagnetic and magnetic semiconductors.[5,6] The utilization of Zener tunneling in structures based on epitaxially grown III-V dilute magnetic semconductors (DMS) is a necessary logical step in designing all-semiconductor spin-injection devices. Indeed, it has been proven experimentally that the electrons in III-V semiconductors have remarkably long spin lifetimes while the holes tend to rapidly dissipate their spin.[7] Therefore, for futher spin manipulations, one needs the spin-polarized electrons rather than the holes, while to date all known III-V DMS are *p*-type. The first spin-injection devices (Esaki diodes) based on Zener tunneling of valence electrons from *p* type ferromagnetic GaMnAs into *n*-GaAs have been already fabricated and successfully tested.[5,6]

In this paper we consider theoretically another type of system that utilizes spin-dependent *resonant* tunneling in magnetic heterostructures with type-II broken-gap band alignment. These systems are resonant interband tunneling devices (RITD) based on InAs/AlSb/GaMnSb/AlSb/InAs double-barrier hetorostructures (DBH). A schematic band diagram of such a DBH is shown in the inset to Fig. 1. The band offset between InAs and GaMnSb leaves a ~ 0.15–0.2 eV energy gap between the bottom of the conduction band in InAs and top of valence band in GaMnSb.[8,9] Therefore the electrons from InAs emitter can tunnel through the hole states in the GaMnSb quantum well into InAs collector. Since the quantized hole states in the quantum well are spin polarized, the emerging electrons are expected to be spin polarized as well. Previous investigations of conventional (i.e., spin-independent) interband resonant tunneling have been mainly focused on RITDs with GaSb quantum wells[8,10] or similar devices[11–13] and revealed quite robust operation in a wide temperature range.

The spin-filtering effect, or more precisely, the exchange splitting of the light-hole channel has been observed experimentally in DBH with semimetallic ErAs quantum wells.[14] The band diagram of the ErAs-based system is similar to that of the proposed GaMnSb-based DBH, with the latter having an obvious advantage of being ferromagnetic rather than paramagnetic. $Ga_{1-x}Mn_xSb$ random alloys with Curie temperature $T_c \sim 25$–30 K have been grown and characterized.[15] Recently, much higher T_C has been reported for $Ga_{1-x}Mn_xSb$ digital alloys.[16] At the same time, digital growth techniques are proven to be very efficient for growing high-quality magnetic quantum wells.[17] This makes manufacturing of GaMnSb-based spin RITD a technological reality.

To describe spin-dependent interband resonant tunneling in GaMnSb-based DBH, we use standard 8×8 $\mathbf{k}\cdot\mathbf{p}$ Kane Hamiltonians in the nonmagnetic InAs and AlSb regions[18] and a generalized Kane Hamiltonian which accounts for magnetism in $Ga_{1-x}Mn_xSb$ quantum well:

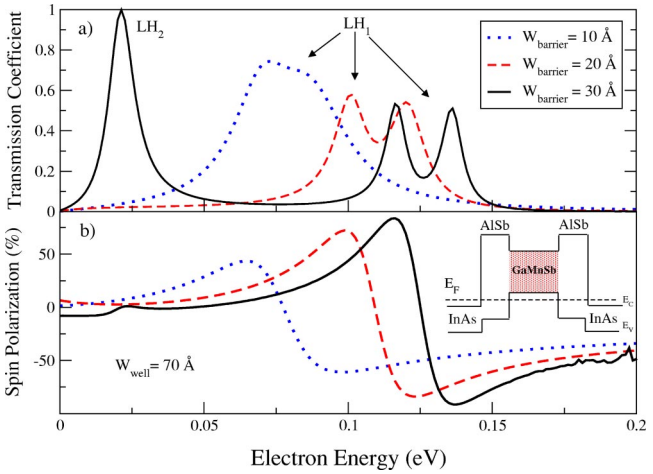

FIG. 1. (a) (Color online) Transmission coefficients of InAs/AlSb/GaMnSb heterostructure with 70-Å quantum well and various barrier widths; (b) perpendicular single-electron spin polarizations at $\vec{k}_{\parallel}=0$.

$$H=\left(E_g+\frac{\hbar^2k^2}{2m^*}\right)\mathcal{P}_e+\mathcal{P}_h\overline{H}_h(\vec{k})\mathcal{P}_h+p\sum_{\sigma=\pm1,\alpha=x,y,z}(k_\alpha|\alpha\sigma\rangle\times\langle s\sigma|+\text{H.c.}) \quad (1)$$

Hamiltonian (1) operates in eight-dimensional Hilbert space spanned by the basis vectors $|s\sigma\rangle$ and $|\alpha\sigma\rangle$ ($\alpha=x,y,z$) of the lower conduction (s-like) and upper valence (p-like) states at the Brillouin-zone center. Here $\mathcal{P}_e=\Sigma_\sigma|s\sigma\rangle\langle s\sigma|$ and $\mathcal{P}_h=\Sigma_{\sigma,\alpha}|\alpha\sigma\rangle\langle\alpha\sigma|$ are the projectors onto the electron and hole subspaces, respectively, p is the Kane matrix element, which is related to another more commonly used parameter E_p as $p^2=\hbar^2E_p/2m_0$ (m_0 is the free-electron mass). The second term in Eq. (1) describes a modified ''Kohn-Luttinger–exchange'' hole Hamiltonian with

$$\overline{H}_h(\vec{k})=-(\overline{\gamma}_1+4\overline{\gamma}_2)k^2+6\overline{\gamma}_2\sum_\alpha L_\alpha k_\alpha^2+6\overline{\gamma}_3\sum_{\alpha\neq\beta}[L_\alpha L_\beta]_+k_\alpha k_\beta+\frac{1}{3}\Delta_{so}(\vec{L}\cdot\vec{\sigma}-1)+\frac{1}{2}\Delta_{ex}(\vec{\sigma}\cdot\hat{m}), \quad (2)$$

where $\vec{\sigma}\equiv(\sigma_x,\sigma_y,\sigma_z)$, σ_α and $\hbar L_\alpha$ are Pauli spin opertaors and orbital angular momentum operators, respectively, $[L_\alpha L_\beta]_+=L_\alpha L_\beta+L_\beta L_\alpha$, Δ_{so} is the valence-band spin-orbit splitting at $\vec{k}=0$, $\hat{m}$ is the unit vector in the direction of magnetization, Δ_{ex} is the exchange splitting at $\vec{k}=0$, and we assume that z axis is perpenicular to the layers. We will consider only saturation magnetizations where $\Delta_{ex}=(5/2)\beta N_0x$. Here β is the p-d exchange coupling constant, N_0 is the number of cations per unit volume in $Ga_{1-x}Mn_xSb$ and x is Mn concentration. The numerical value of $\Delta_{ex}\simeq90$ meV at $x=0.05$ is consistent with the Curie temperature of bulk GaMnSb,[15,19] $T_c\simeq25$–30 K. The renormalized Luttinger parameters $\overline{\gamma}_i$ and the mass parameter m^* are related to the electron effective mass m_e and to the valence-band Luttinger parameters γ_i in a standard way.[20] We fitted the bands in bulk InAs, AlSb, and GaSb by means of the sets of parameters m_e, γ_i,[9,18] and fixed $E_p=21$ eV.

To calculate the transmission coefficient we will use the transfer-matrix technique[21] and represent the device as a stack of two-dimensional flat-band interior layers with thickness $w_n=z_n-z_{n+1}$ and an average electrostatic potential $-eV_n$ starting at $z=z_0=0$ and ending at $z=z_N$, where z_N is the length of the device. The $0_{th}\equiv L$ and $(N+1)_{th}\equiv R$ layers are semi-infinite InAs emitter ($z<0$) and collector ($z>z_N$) having electrostatic potentials $V_0=0$ and $-eV_{N+1}=-eV$, respectively, where V is the bias applied to the structure. We will take into account elastic processes only, i.e., assume that the electron energy E and lateral momentum $\vec{k}_\parallel$ are conserved. Substituting $k_z\to-i\partial/\partial z$ into the Kane Hamiltonian matrix we can transform it into a quadratic form $H=H^{(2)}(-i\partial/\partial z)^2+H^{(1)}(-i\partial/\partial z)+H^{(0)}$, where $H^{(i)}$ are 8×8 Hermitian matrices depending on $\vec{k}_\parallel$, and solve Schrödinger's equation in the n_{th} flat-band region:

$$\overline{\Psi}_n(z)=\sum_{\alpha=1}^{8}[A^+_{n\alpha}\overline{v}(k^+_{n\alpha})e^{ik^+_{n\alpha}z}+A^-_{n\alpha}\overline{v}(k^-_{n\alpha})e^{ik^-_{n\alpha}z}], \quad (3)$$

where $\overline{\Psi}$ and $\overline{v}$ are eight-component column vectors and we separated all our solutions into two subsets with k^+_α corresponding to either traveling waves carrying the probability current from left to right or to evanescent waves decaying to the right and k^-_α corresponding to their left counterparts. Since the Kramers symmetry is broken in the magnetic part of the device $k^+_\alpha\neq-k^-_\alpha$ for real k (traveling waves), however, complex k always occur in complex conjugated pairs, i.e., $k^+_\alpha=k^-_\alpha{}^*$. The latter condition is a consequence of the Hermitian character of the matrices $H^{(i)}$. This condition is necessary to ensure that the current across the device is steady state. The technique of finding eigenvalues $k^\pm_{n\alpha}$ and eigenvectors $\overline{v}(k^\pm_{n\alpha})$ is described in Refs. 8,21. Using these quantities and the matching conditions,[8,21,22] ensuring the continuity of the wave function and the current across the device, we can construct the transfer matrix M which relates the wave-function amplitudes in the emitter and collector:

$$\begin{pmatrix}A^+_L\\A^-_L\end{pmatrix}=\begin{pmatrix}M_+&M_{+-}\\M_{-+}&M_-\end{pmatrix}\begin{pmatrix}A^+_R\\0\end{pmatrix} \quad (4)$$

The 16×16 matrix M in Eq. (4) is partitioned in such a way that M_+ provides the relation between the amplitudes of the incident waves in the emitter A^+_L and the transmitted waves A^+_R in the collector.

For any $k_\parallel$, E, and $-eV$, the 8×8 transfer matrix M_+ can be found and the transmission matrix can be calculated straightforwardly:

$$t_{\alpha\beta}=\begin{cases}\sqrt{j_{R\beta}/j_{L\alpha}}(M_+)^{-1}_{\beta\alpha} & \text{if} \quad j_{L\alpha(R\beta)}>0 \quad \text{and} \quad \text{Im}k_{L\alpha(R\beta)}=0\\ 0, \quad \text{otherwise,}\end{cases} \quad (5)$$

where $j_{L\alpha}$ and $j_{R\beta}$ are the expectation values of the multiband probability current operator for the electron in the input channel α and the output channel β, respectively,[8,21] $\hbar j_{L\alpha}=\text{Re}\langle\overline{v}^\dagger(k_{L\alpha})|2H^{(2)}k_{L\alpha}+H^{(1)}|\overline{v}(k_{L\alpha})\rangle$, and $j_{R\beta}$ is defined similarly. The transmission coefficient $T(\vec{k}_\parallel,E,eV)$ and spin transmissivity $\vec{\mathcal{S}}(\vec{k}_\parallel,E,eV)$[23] can be calculated as well:

$$T(\vec{k}_\parallel, E, eV) = \frac{1}{2}\mathrm{Tr}(t \cdot t^\dagger), \tag{6}$$

$$\vec{\mathcal{S}}(\vec{k}_\parallel, E, eV) = \frac{1}{2}\mathrm{Tr}(t \cdot \vec{\sigma} \cdot t^\dagger). \tag{7}$$

The transmission coefficients for InAs/AlSb/GaMnSb DBH with 70-Å-wide quantum well and 10-, 20-, and 30-Å-wide barriers are shown in Fig. 1(a). The magnetization is saturated and directed along *z* axis, i.e., perpendicular to the layers. The spin splitting of the LH channels is well pronounced for the structure with wider barriers (20 and 30 Å). It is weakly resolved as a shoulder for the structure with 10-Å barriers. The barrier width, which is responsible for the width of the spin-resolved peaks is therefore one of the critical parameters for the structures in question. This observation is well supported by the calculated single-electron perpendicular spin polarizations $\mathcal{S}_z/T$ at $k_\parallel = 0$, shown in Fig. 1(b) for 70-Å-wide quantum well and 10-, 20-, and 30-Å-wide barriers. The maximum value of *p* is 60% for the structure with 10-Å barriers, while for the structure with 30-Å barriers it reaches 95%.

Similar to the conventional InAs/GaSb RITD, the heavy hole (HH) resonant peaks are absent at $\vec{k}_\parallel = 0$. For perpendicular (or zero) magnetization and a tunneling electron with $k_\parallel = 0$, the *z* component of the total angular momentum, J_z, is a good quantum number and, therefore, must be conserved. Thus, tunneling of *s* electrons near the conduction-band minimum of InAs with $J_z = \pm 1/2$ through the hole states with $J_z = \pm 3/2$ is prohibited. Such a possibility exists for either finite $k_\parallel$ or in-plane magnetization. As we will see below, the former is rather insignificant while the latter affects the interband resonant tunneling in a drastic way. For better insight we will treat our system by means of the tunneling Hamiltonian formalism,[24] which gives an analytical expression for the transmission coefficient at $\vec{k}_\parallel = 0$. In this framework the system is described by two coupled Schrödinger equations:

$$H^e_\sigma |\psi^e_\sigma\rangle + \sum_m \hat{V}_{\sigma m} |\varphi^h_m\rangle = E |\psi^e_\sigma\rangle, \tag{8}$$

$$\sum_{m'} H^h_{mm'} |\varphi^h_{m'}\rangle + \sum_\sigma \hat{V}_{m\sigma}{}^\dagger |\psi^e_\sigma\rangle = E |\varphi^h_m\rangle, \tag{9}$$

Equation (8) describes an electron with spin $\sigma = \pm 1/2$ tunneling through the potential barrier (evanescent channel) which is coupled with the confined hole states φ^h_m by a mixing potential $\hat{V}_{\sigma m}$. The basis of the localized hole states $|\varphi^h_m\rangle$ is defined in terms of spherical harmonics with *m* being the *z* projection of the angular momentum onto the interface normal. Thus matrix $H_{mm'}$ is nondiagonal for an arbitrary orientation of the magnetization with respect to the interface. At $\vec{k}_\parallel = 0$ the operator $\hat{V}_{\sigma m} = -ip\delta_{\sigma,m}\partial/\partial z$. Since H^e_σ has continuous spectrum the situation is typical for the appearance of Fano resonances.[25]

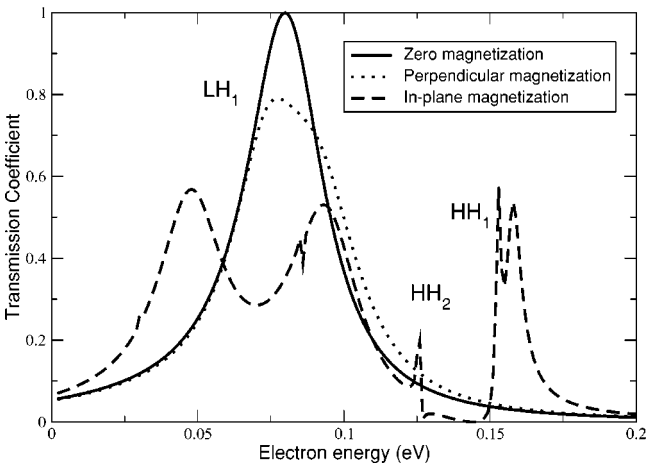

FIG. 2. Transmission coefficients of InAs/AlSb/GaMnSb DBH with 70-Å quantum well and 10-Å barriers ($\vec{k}_\parallel = 0$).

We will concentrate on the two particularly important cases of magnetization perpendicular and parallel to the layers. Taking into account only the first two quantized hole levels $E_{1/2}$ (light hole) and $E_{3/2}$ (heavy hole) and assuming that the barrier is symmetric (i.e., $eV = 0$), we obtain the following expression for the transmission coefficient at $k_\parallel = 0$:

$$T_{\hat{m}}(E) = \frac{1}{2} T_0 \sum_{\sigma=\pm 1} \frac{(\Sigma^\sigma_{\hat{m}}(E) + \Delta_E)^2}{[\Sigma^\sigma_{\hat{m}}(E) + \Delta_E - \Gamma_E \sqrt{R_0/T_0}]^2 + \Gamma_E^2}, \tag{10}$$

where $T_0 = |t_0|^2$ and $R_0 = 1 - T_0$ are the "bare" transmission and reflection coefficients, describing nonresonant and spin-independent electron tunneling in the absence of the mixing potential, and the self-energy $\Sigma^\sigma_{\hat{m}}(E)$ is given by

$$\Sigma^\sigma_{\hat{m}}(E) = \left\{ \begin{array}{ll} E - E_{1/2} - \frac{1}{2}\sigma\Delta_{ex}, & \hat{m} \| z \\ E - E_{1/2} - \sigma\Delta_{ex} - \frac{3\Delta^2_{ex}}{4(E - E_{3/2})}, & \hat{m} \| x. \end{array} \right\} \tag{11}$$

Here we have introduced the inverse elastic lifetime of the light-hole state $\Gamma_E \propto p^2$ and its energy shift due to the mixing potential $\Delta_E \propto p^2$. The expressions for Γ_E and Δ_E can be obtained straightforwardly, however, they are rather cumbersome and not important for our analysis. The only fact which is important is that both Γ_E and Δ_E are decreasing functions of the barrier width.

Equation (11) allows for rather meaningful and physically transparent interpretation of the transmission coefficient, calculated numerically by means of the transfer-matrix technique (Fig. 2). First of all we note that Eq. (11) describes a series of Fano resonances and antiresonances.[25–27] In the absence of the magnetization, $\Sigma_+(E) = \Sigma_-(E) = \Sigma(E)$ and we have only one resonance $[T(E) = 1]$ at $\Sigma + \Delta_E = (\Gamma_E/2)\sqrt{T/R}$ and antiresonance $[T(E) = 0]$ at $\Sigma(E) + \Delta_E = 0$, both corresponding to the light-hole channel. When the

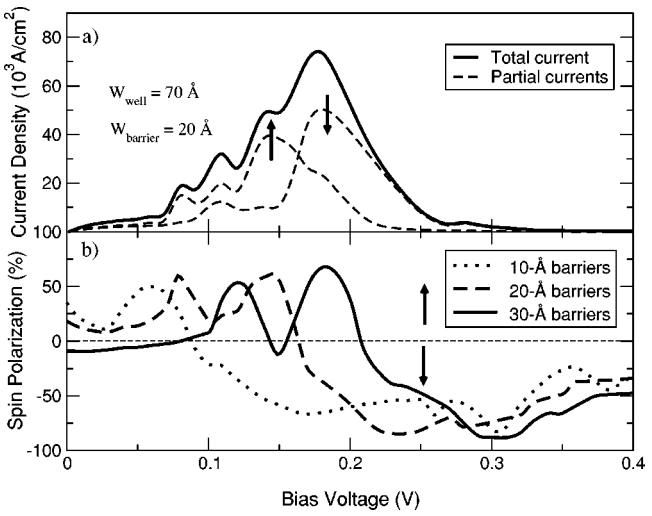

FIG. 3. (a) *I-V* curve for InAs/AlSb/GaMnSb DBH with 70-Å quantum well, 20-Å barriers, and perpendicular magentization; (b) bias dependence of the current spin polarization $j_{s,z}/j$ for 70-Å quantum well, various barriers, and perpendicular magnetization.

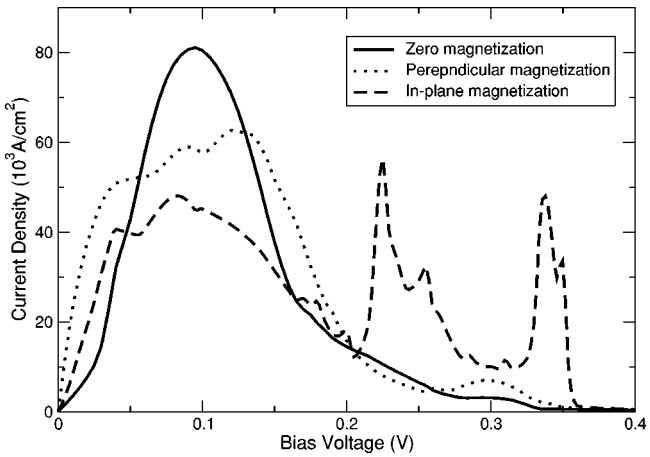

FIG. 4. *I-V* charactersitics of InAs/AlAs/GaMnSb DBH with 70-Å quantum well and 10-Å barriers, for zero, perpendicular, and in-plane magnetizations in the quantum well.

magnetization $\vec{M}$ is perpendicular to the layers, the light-hole (LH) resonance is exchange split, which leads to the perpendicular spin polarization of the transmitted electron wave. Finally, the in-plane magnetization splits LH channel even more strongly and induces another resonance-antiresonance pair corresponding to the HH channel. This channel, which is completely invisible for zero or perpendicular magnetization, becomes very pronounced when $\vec{M}$ is in plane. This is a direct manifestation of the angular momentum selection rules combined with the exchange enhancement of the effective g factor due to the localized Mn spins in the quantum well.[28,29]

We now turn to a calculation of charge j and spin $\vec{j}_s$ current densities:[30]

$$j=\frac{e}{2\pi^2 h}\int\int d\vec{k}_{\parallel}dE[f(E)-f(E+eV)]T(\vec{k}_{\parallel},E,eV), \tag{12}$$

$$\vec{j}_s=\frac{e}{2\pi^2 h}\int\int d\vec{k}_{\parallel}dE[f(E)-f(E+eV)]\vec{\mathcal{S}}(\vec{k}_{\parallel},E,eV), \tag{13}$$

where $f(E)$ is the Fermi function. Current-voltage characteristics calculated for $T=4$ K, 20-Å barriers and a 70-Å quantum well are shown in Fig. 3(a). The current is calculated for perpendicular magnetization and the Fermi energy $E_F=0.04$ eV, which corresponds to electron concentration in InAs $n\sim 10^{18}\,cm^{-3}$, and 0.1 hole per Mn ion in the $Ga_{1-x}Mn_xSb$ quantum well at $x=0.05$. The exchange splitting of the LH channel is resolved as a shoulder on the total current curve, which is a superposition of two very distinct partial spin-up and spin-down currents. This suggests that perpenicular spin polarization $j_{s,z}/j$ of the tunneling current must be quite significant [Fig. 3(b)]. In this particular case (20-Å barriers) $j_{s,z}/j$ reaches 90%. The most striking result of our calculations is a sharp dependence of spin polarization on the applied bias. As follows from Fig. 3(b), one can drastically change both magnitude and sign of $j_{s,z}/j$ by applying external voltage. Such controllable spin filtering is a remarkable feature of magnetic RITD and may have significant potential for a variety of possible spin-injection applications.[31] Since the spin-split channels are better resolved for the structures with wider barriers (Fig. 1) the spin polarization of the tunneling current is also higher for these structures. However, this effect is not as strong as we might expect, and the highest polarization values for different barrier widths are rather similar [Fig. 3(b)].

As we already mentioned, the in-plane magnetization affects resonant tunneling in a dramatic way (Fig. 2). Figure 4 shows three current-voltage characteristics for zero, perpendicular, and parallel magnetizations, calculated for $T=4$ K and the structure with 70-Å quantum well and 10-Å barriers. The zero magnetization curve is similar to that of the conventional RITD and displays a very strong LH resonant channel and a very weak feature stemming from the first HH state in the quantum well. The same is true for the perpendicular magnetization where the LH channel is split into spin-up and spin-down subchannels but the HH peak remains very weak. The most drastic changes of the *I-V* characteristics occur for the in-plane magnetization where, along with the splitting of the light-hole channel, two new peaks related to the heavy-hole states in the quantum well emerge. This effect is due to the mixing of the LH and HH channels at $\vec{k}_{\parallel}\simeq 0$, which results in the lifting of the angular momentum selection rules.[28] The induced heavy-hole resonant channels have been clearly observed in resonant tunneling through paramagnetic ErAs quantum wells in saturating in-plane magnetic fields.[14] Even though nonzero $k_{\parallel}$ in the cases of perpendicular and zero magnetization also allows for tunneling of the electrons through the heavy-hole states, the corresponding resonances are rather weak, and are almost completely washed out by the integration over $k_{\parallel}$ in Eq. (12) (see also Ref. 8).

This work was supported by the NSF Grant No. DMR-0071823 and by NRL under ASEE-NAVY Summer Faculty Program. We are grateful to Berry Jonker and Steve Erwin for fruitful discussions.

*Present address: Physics Department, Georgetown University, Washington, DC 20057.
†Present address: Department of Chemical and Materials Engineering, Arizona State University, Tempe, AZ 85287.

[1] E.I. Rashba, Phys. Rev. B **62**, R16 267 (2000).
[2] H.J. Zhu, M. Ramsteiner, H. Kostial, M. Wassemeier, H.-P. Schonherr, and K.H. Ploog, Phys. Rev. Lett. **87**, 016601 (2001).
[3] A.T. Hanbicki, B.T. Jonker, G. Itskos, G. Kioseoglou, and A. Petrou, Appl. Phys. Lett. **80**, 1240 (2002).
[4] T. Koga, J. Nitta, H. Takayanagi, and S. Datta, Phys. Rev. Lett. **88**, 126601 (2002).
[5] M. Kohda, Y. Ohno, K. Takamura, F. Matsukura, and H. Ohno, Jpn. J. Appl. Phys., Part 1 **40**, L1274 (2001).
[6] E. Johnston-Halperin, D. Lofgreen, R.K. Kawakami, D.K. Young, L. Coldren, A.C. Gossard, and D.D. Awschalom, Phys. Rev. B **65**, 041306 (2002).
[7] J.M. Kikkawa and D.D. Awschalom, Nature (London) **397**, 139 (1999).
[8] Y.X. Liu, R.R. Marquardt, D.Z.-Y. Ting, and T.C. McGill, Phys. Rev. B **55**, 7073 (1997).
[9] P.S. Dutta and H.L. Bhat, J. Appl. Phys. **81**, 5821 (1997).
[10] R.R. Marquardt, D.A. Collins, Y.X. Liu, D.Z.-Y. Ting, and T.C. McGill, Phys. Rev. B **53**, 13 624 (1996).
[11] E.E. Mendez, J. Nocera, and W.I. Wang, Phys. Rev. B **45**, 3910 (1992).
[12] E.E. Mendez, Surf. Sci. **267**, 370 (1992).
[13] T. Takamasu *et al.*, Surf. Sci. **263**, 217 (1992).
[14] D.E. Brehmer, K. Zhang, C.J. Schwarz, S.P. Chau, and S.J. Allen, Appl. Phys. Lett. **67**, 1268 (1995).
[15] F. Matsukura, E. Abe, and H. Ohno, J. Appl. Phys. **87**, 6442 (2000).
[16] X. Chen *et al.*, Appl. Phys. Lett. **81**, 511 (2002).
[17] S.A. Crooker, D.A. Tulchinsky, J. Levy, D.D. Awschalom, R. Garcia, and N. Samarth, Phys. Rev. Lett. **75**, 505 (1995).
[18] D.N. Talwar, J.P. Loehr, and B. Jogai, Phys. Rev. B **49**, 10 345 (1994).
[19] T. Dietl, H. Ohno, F. Matsukura, J. Cibert, and D. Ferrand, Science **287**, 1019 (2000).
[20] T.E. Ostromek, Phys. Rev. B **54**, 14 467 (1996).
[21] A.G. Petukhov, A.N. Chantis, and D.O. Demchenko, Phys. Rev. Lett. **89**, 107205 (2002).
[22] C.Y. Chao and S.L. Chuang, Phys. Rev. B **43**, 7027 (1991).
[23] J.C. Slonczewski, Phys. Rev. B **39**, 6995 (1989).
[24] S.A. Gurvitz and Y.B. Levinson, Phys. Rev. B **47**, 10 578 (1993).
[25] U. Fano, Phys. Rev. **124**, 1866 (1961).
[26] R.C. Bowen, W.R. Frensley, G. Klimeck, and R.K. Lake, Phys. Rev. B **52**, 2754 (1995).
[27] G. Klimeck, R.C. Bowen, and T.B. Boykin, Superlattices Microstruct. **29**, 187 (2001).
[28] A.G. Petukhov, W.R.L. Lambrecht, and B. Segall, Phys. Rev. B **53**, 3646 (1996).
[29] A.G. Petukhov, Appl. Surf. Sci. **123/124**, 385 (1998).
[30] C.B. Duke, *Tunneling in Solids* (Academic, New York, 1969).
[31] G.A. Prinz, Science **250**, 1092 (1990).